Journal of Mathematical Chemistry Vol. 35, No. 3, March 2004 (© 2004)

A three-state model for electronic transitions represented in a generalized diabatic approach

Gustavo A. Arteca*

Department of Physical Chemistry, Uppsala University, Box 579, S-751 23 Uppsala, Sweden and Département de Chimie et Biochimie, Laurentian University, Ramsey Lake Road, Sudbury, Ont., Canada P3E 2C6
E-mail: gustavo@laurentienne.ca

O. Tapia

Department of Physical Chemistry, Uppsala University, Box 579, S-751 23 Uppsala, Sweden

Received 3 November 2003; revised 9 March 2004

We describe the chemical change between two diabatic closed-shell states as an electronic transition mediated by two factors: a bound diabatic transition state and the electromagnetic field. Using a three-state model for bond breaking, we compute the amplitudes of the total quantum state on the diabatic reactant, product, and transition states as a function of the external field. Changes in the total electronic state appear as sharp transitions between diabatic basis functions for particular configurations of the set of external positive charges. Depending on the diabatic states and the external field, the model predicts the possible occurrence of energy barriers for breaking or forming covalent bonds.

KEY WORDS: Diabatic functions, quantum-state transitions, reaction barners

AMS subject classification: 81V55, 81S99

1. Introduction

It is well known that the adiabatic approach for chemical reactions breaks down not only in cases involving excited or ionic species but also for ground states at room temperature [1,2]. The shortcomings of the method stem from the fact that, within the Born–Oppenheimer (BO) approximation, chemical processes are viewed as occurring on the single potential energy hypersurface of an *isolated* molecular system; on that surface, electronic configurations appear to change smoothly (and spontaneously) as the nuclei move. The BO approach fails if two adiabatic surfaces are near each other. This situation is not only common (e.g., it occurs often at standard harmonic transition structures), but also is

* Corresponding author.

0259-9791/04/0300-0159/0

known to make a large contribution to inelastic and elastic transitions [3]. Compounding this drawback, the standard approach to studying adiabatic surfaces for isolated molecular systems omits the explicit role of the electromagnetic field as the actual driver for transitions in the quantum states.

To address these issues, a number of alternative nonadiabatic approaches have become computationally available in recent years (see [1,4–7], and references cited therein). Presently, we leave aside methods involving post-BO nuclear dynamics [7]; our goal is to describe electronic transitions in cases where one can *externally* manipulate the geometrical arrangement of positive (nuclear) charges. Common approaches relevant to the present work follow two routes: (a) introducing nonadiabatic couplings between adiabatic basis functions (e.g., using the nuclear momentum operators on electronic wave functions [4]), and (b) representing electronic wave functions using *diabatic* (or "dynamic") *states* [3–6].

The definition and properties of diabatic states have been subject to considerable debate [1,5,6,8]. Even though it is agreed that diabatic functions should conserve an electronic configuration with respect to smooth changes in nuclear geometry, there are several possible definitions for such states [3,5,6,8]. In our view, there is still no satisfactory method for representing electronic quantum states with diabatic basis functions in such a way that chemical processes emerge as transitions driven by an external electromagnetic field. In this work, we propose a methodology with these characteristics, and illustrate its application with a model for the transitions between two closed-shell states. We refer to the method as the generalized electronic diabatic (GED) approach. We focus on outlining qualitatively the physical process associated with changes in quantum states. For the present work, we simply consider that there exists a diabatic set of electronic functions. We make no attempt to discuss the actual construction of these functions, but rather discuss consequences resulting from their existence. In particular, we highlight the role played by states (TSs) as necessary players in some of electronic transitions.

In the present GED approach, electronic (molecular) quantum states are linear superpositions of diabatic electronic states. Each diabatic function describes one electronic configuration (or a "single chemical species"), regardless of the geometry of the "external" background of positive charges (e.g., the nuclei) embedded in the electron density [9,10]. We assume that the geometry of the positive-charge background can be modified externally, as one would with massless classical test charges. As stated before, we make no assumptions with respect to nuclear mass dynamics, but focus instead on how electronic transitions occur while the charge configuration in laboratory space is modified within an external field. The resulting total quantum states depend on this field and on the charge configuration through the coefficients of the linear superposition, and not through the diabatic functions themselves.

The work is organized as follows. First, we discuss briefly the diabatic representation in terms of a unique complete set of orthogonal eigenfunctions of

a fixed-point hamiltonian. The actual electronic quantum state for the molecule is then built using the diabatic basis set. Second, we use this method to build a minimalist model for bond breaking/formation. For illustration, we discuss bond breaking in a closed-shell diatomic molecule, a case which requires three states: the *close-shell singlet states* for the reactant and the product, and an *open-shell singlet* for a transition state. In the GED approach, the latter is required to mediate the chemical reaction; however, the transition state appears in the diabatic representation as a standard *bound state*, and not as a saddle point on a single adiabatic hypersurface. Using a simple representation for the diabatic potential energy functions, we apply the three-state model to study how the *quantum process* of chemical change is affected by internal and external factors. Depending on the diabatic transition state and the strength of the applied field, we discuss how the contribution of reactants and products to the energy of quantum state may, or may not, result in an effective barrier. Conclusions appear in the last section.

2. The generalized electronic diabatic basis set and general quantum states

The starting point for our analysis is to divide a molecule into a quantum subsystem (the n electrons) and a classical one (a set of m massless positive charges). We assume that the latter can be externally manipulated at will in the three-dimensional laboratory space for the m charges, $\Re^{3m}$; all possible configurations in $\Re^{3m}$ are considered to be accessible to any electronic state. We work under the principle that *stationary* electronic states are represented by *diabatic functions*, which are *independent* of the configuration of the positive-charge background. Although these wave functions are configuration-independent, each produces a potential energy function that changes, in general, with the electronic state. As a hypothesis, we assume that the resulting diabatic potential energy functions are *confining attractors*, i.e., each diabatic function determines a *single stationary configuration* for the background of positive charges [10]. When measured from a fixed laboratory frame $\Re^{3m}$, the stationary configurations may appear as finite-length vectors (a "molecular geometry") or infinity-length vectors (an asymptotic geometry with "broken bonds"). In both cases, however, the diabatic potential energy will increase as one moves away from the stationary geometry. Two important conceptual distinctions must be stressed with respect to the standard adiabatic approach [1] and alternative diabatic methods [3–8, 11–13]. First, the present basis functions do not change with the nuclear geometry as they would in the BO approximation. Second, the present basis set of diabatic functions is derived from a fixed-point hamiltonian associated with a stationary geometry for the positive charges; yet, the resulting set of functions is the same, *regardless* of which stationary geometry is chosen. From now on, we

assume that a basis set with these characteristics exists, and then proceed on to derive a number of consequences.

Let us consider a neutral molecular system, comprising n electrons embedding a background of m "external" positive charges. We discuss presently the case where the dynamics of the *classical* positive charges is controlled *externally*. The actual dynamics of nuclear masses [7] could be introduced at a later stage, if desired, through a normal-mode analysis on the potential energy functions discussed below.

The "external potential" associated with the background of m positive charges is characterized by two vectors, $\mathbf{Z} = (Z_1, \ldots, Z_m)$ and $\xi = (\xi_1, \ldots, \xi_m)$, corresponding to the charges' value (in units of $|e|$) and physical location. We denote the nuclear charge configuration by ξ, to stress the distinction with the standard $\mathbf{R}$ used to the indicate instantaneous position of the nuclear *masses* in the BO approximation. Let $|\Psi\rangle$ denote the quantum state for an n-electron system with an external potential in configuration ξ. Leaving spin aside for the moment, this state is completely specified by a *diabatic* function $\Psi(\mathbf{q})$, where $\mathbf{q} = (q_1, \ldots, q_n)$ is a configuration in the $\Re^{3n}$-space supporting the Hilbert space. The hamiltonian for this quantum/classical system is independent of nuclear masses:

$$H_e(\mathbf{q}, \xi) = K_e(\mathbf{q}) + V_C(\mathbf{q}, \xi), \tag{1}$$

with $K_e(\mathbf{q})$ the electronic kinetic energy operator and $V_C(\mathbf{q}, \xi)$ the Coulomb potential for *all* (quantum and classical) charges. To any electronic state $\Psi_k(\mathbf{q})$, we associate an expectation value, or diabatic potential energy function, U_k, that is a function of ξ and functional of Ψ:

$$U(\xi; [\Psi_k]) = \langle \Psi_k(\mathbf{q}) | H_e(\mathbf{q}, \xi) \Psi_k(\mathbf{q}) \rangle_q. \tag{2}$$

In a bound state, U_k will increase monotonically from a minimum value, despite the fact that $\Psi_k(\mathbf{q})$ is independent of ξ. We shall now require that the functional (2) be stationary with respect to displacements of the positive charge background from a configuration ξ^k:

$$\left\| \left(\frac{\partial U_k}{\partial \xi} \right) \Big|_{\xi^k} \right\| = 0. \tag{3}$$

The vector ξ^k can be thought as a label that characterizes an electronic system at a diabatic state $|\Psi_k\rangle$. Moreover, if we require that U_k also be stationary with respect to $\mathbf{Z}$, we obtain a family of actual chemical species consistent with the electronic information contained in $\Psi_k(\mathbf{q})$. In particular, $|\Psi_1\rangle$ will denote the ground state. Note that the resulting $\Psi_k(\mathbf{q})$ are the exact eigenfunctions of $H_e(\mathbf{q}, \xi)$; these functions satisfy properties (including orthogonality, see below) that are not be guaranteed when using approximate solutions, e.g. Hartree–Fock.

Now, we know that the molecular operator $H_e(\mathbf{q}, \xi)$ is *essentially self-adjoint* [14], i.e., it has a complete set of eigenfunctions. Since this property is independent of the terms retained in the Coulomb potential [14], we can then extract a complete set of diabatic eigenfunctions from the *fixed-point* hamiltonian $H_e(\mathbf{q}, \xi^k)$ at any stationary configuration ξ^k. Accordingly, a diabatic basis set $\{\Psi_s(\mathbf{q})\}$ is obtained by requiring that the functional (2) be a minimum over variations in wave function space, $\delta_\Psi\{U(\xi^k; [\Psi])/\|\Psi\|^2\} = 0$, leading to [10]:

$$H_e(\mathbf{q}, \xi^k)\Psi_s(\mathbf{q}) = E_s(\xi^k)\Psi_s(\mathbf{q}) = U(\xi^k; [\Psi_s])\Psi_s(\mathbf{q}), \tag{4}$$

with the understanding that the resulting $\{\Psi_s(\mathbf{q})\}$-set is *universal*, in the sense that the *same* functions will be obtained if any other stationary-point hamiltonian is used. Moreover, since each $U(\xi; [\Psi_s])$ functional is a distinct single-minimum attractor, the diabatic functions will be orthogonal, except for accidental degeneracies. We note also two implications from equations (2–4): (i) $U(\xi^1; [\Psi_1])$ is the global minimum of $U(\xi; [\Psi])$ in configurational space ($\Re^{3m}$) and in Hilbert space; (ii) The solution of equation (4) is iterative, since we need the Ψ_k-function to get the ξ^k configuration required to build the fixed-point hamiltonian with $\{\Psi_s(\mathbf{q})\}$ eigenfunctions.

Note that, even though the choice of ξ^k does not affect the basis functions, it *will* affect the eigenvalue spectrum $\{E_s(\xi^k)\}$. For example, if we solve equation (4) at the stationary configuration ξ^1 for the (bound) ground state of a diatomic molecule, the diabatic functions for the channels corresponding to the asymptotic dissociation into atoms will also be obtained, but they will appear at high energies. Similarly, the molecular diabatic ground state will also be found, although at infinitely high energies, if sought among the solutions of equation (4) with ξ^k the attractor corresponding to the dissociation into atoms.

The diabatic functions $\{\Psi_s(\mathbf{q})\}$ represent the exact electronic states of the *isolated* quantum/classical system. In addition to being orthogonal eigenfunctions of $H_e(\mathbf{q}, \xi^k)$, the symmetry of $V_C(\mathbf{q}, \xi)$ implies that they also diagonalize the entire molecular hamiltonian: $\langle\Psi_k(\mathbf{q})|H_e(\mathbf{q}, \xi)\Psi_s(\mathbf{q})\rangle_q = 0$, with $k \neq s$. In other words, diabatic states are uncoupled for all ξ-configurations unless the system becomes *nonisolated* by adding an external electromagnetic field [15]. In this case, the general quantum states $|\Phi\rangle$ will be solutions of the extended eigenvalue equation:

$$(H_e(\mathbf{q}, \xi) + V_{e-rad})\Phi(\mathbf{q}) = \varepsilon(\xi)\Phi(\mathbf{q}), \tag{5}$$

where the radiation bath introduces the energy term $V_{e-rad} \simeq \mathbf{A} \cdot \mathbf{p}_e$, with $\mathbf{A}$ the electromagnetic field vector-operator and $\mathbf{p}_e$ the total electronic linear momentum operator (we have omitted the radiation-only term in equation (5)). The $|\Phi\rangle$ states can now be written as a linear combination

$$\Phi(\mathbf{q}; \xi) = \sum_s c_s(\xi)\Psi_s(\mathbf{q}) \tag{6}$$

of diabatic functions. The $\{c_s\}$ coefficients for the superposition depend now on the geometry of the positive-charge background, in addition to the intensity of the radiation field. As a result, the wave function $\Phi(\mathbf{q};\xi)$ and the energy $\varepsilon(\xi)$ of the extended molecule-and-radiation system depend parametrically on the configuration ξ. In contrast to the BO approximation, this parametric dependence disappears if there is no external field. Equation (6) plays the role of a generalized multiconfigurational wave function.

According to equations (5) and (6), the electromagnetic field can, in principle, couple diabatic states at any given ξ-configuration of the positive-charge background. If we now move these charges in the laboratory space $\Re^{3m}$, it is possible that transitions among diabatic states will take place, as reflected by changes in the coefficients $\{c_s\}$. Since each diabatic state $|\Psi_k\rangle$ corresponds to a distinct chemical species, sharp changes in c_s would indicate a chemical reaction. Within our approach, these chemical processes resemble Frank-Condon transitions.

For a given type of chemical process, we can build a model system that incorporates the minimum number of diabatic states required for its qualitative description. For instance, consider the case of a reaction where a σ-bond is broken in a closed-shell diatomic molecule. In this case, the reactant can be associated with the diabatic function $|\Psi_1\rangle$ for the bound singlet ground state of the molecule, whereas the product is represented by the diabatic singlet function $|\Psi_2\rangle$ for a pair of two atoms asymptotically separated. This latter state correlates with a doubly excited singlet of the bound molecule. Since these functions have the same parity, it follows that they are uncoupled up to first order also in presence of the radiation field, $\langle\Psi_1|\mathbf{p}_e\Psi_2\rangle_q = 0$. Accordingly, any transition between these states requires not only the external field but also at least one additional diabatic state with different parity. In the present case, the third state $|\Psi_3\rangle$ will be the bound diabatic state involving a single excitation with respect to the ground state. This singly excited state acts accordingly as the *transition state* for the reaction between reactant and product singlets. In contrast, a bond breaking reaction between doublet states in a molecular radical would not require a third state. Here, reactants and products have different parity and can couple directly with each other in presence of the external field.

In Section 3, we discuss in more detail some of the properties of the three-state model, and show the occurrence of sharp transitions between diabatic states.

3. Three-state model for covalent bond breaking

When using the variational function (6), the ξ-dependent hamiltonian in equation (5) provides the amplitudes on the diabatic "axes" needed to monitor quantum transitions. Here, we deal with a three-state function, where c_1, c_2, and

c_3 are the coefficients for the reactant, product, and TSs, respectively. In order to model a bond-breaking process in a diatomic molecule, we choose for the sake of simplicity a single coordinate x; it can be thought as measuring the position of a charge away from the stationary geometry of the confining attractor for the diabatic ground state $|\Psi_1\rangle$. In terms of x, the three diabatic potential energy functions will be represented by curves $U_i(x) = \langle\Psi_i(\mathbf{q})|H_e(\mathbf{q}, x)\Psi_i(\mathbf{q})\rangle_q, i = 1, 2, 3$, with the following properties: (i) $U_1(x)$ is a confining attractor with a minimum at $x = 0$, (ii) $U_2(x)$ is a monotonously decaying function with a minimum at $x \to \infty$ (i.e., an asymptotic single attractor), and (iii) $U_3(x)$ is also a diabatic bound state for the molecule, thus a single attractor with a shifted minimum at x_3. The third state is actually a transition *state*, i.e., a minimum rather than a saddle-point transition structure. These characteristics will persist if we use the three-state model for studying bond breaking in a polyatomic molecule.

Our focus in this section is on the factors that control the transitions between diabatic states, rather than on the diabatic functions themselves. For this reason, we will discuss the behaviour of the $\{c_i(x)\}$ coefficients in equation (6) by using model curves for the diabatic potentials $\{U_i(x)\}$. The three-state model is defined by the dimensionless functions:

$$U_1(x) = k_1 x^2, \tag{7a}$$

$$U_2(x) = \Delta_2 + k_2 \exp(-a_2 x), \tag{7b}$$

$$U_3(x) = \Delta_3 + k_3 (x - x_3)^2. \tag{7c}$$

For the simplest closed-shell diatomics, H_2, the three functions can easily be assigned to electronic states: (a) The $|\Psi_1\rangle$ state corresponds to the *diabatic* ground state singlet, $(\sigma_g)^2$. Since this is a diabatic state, $U_1(x)$ increases monotonically for $x > 0$ and does not lead to dissociation. (b) The $|\Psi_2\rangle$ state corresponds to the *diabatic* doubly excited state, $(\sigma_u)^2$; conveniently scaled, this state has a attractor in the configuration of two hydrogen atoms asymptotically separated. In the standard adiabatic approach, this double excitation appears as a configuration-interaction contribution to the ground state at large interatomic distances. (c) The $|\Psi_3\rangle$ state corresponds to the *diabatic* singly excited singlet, $\sigma_g\sigma_u$. This diabatic state is responsible for the minimum energy geometry of the $B^1\Sigma_u^+$ molecular bound state of H_2 [16]. Below, we monitor how the amplitudes $\{c_i(x)\}$ change as the position of the minimum of $U_3(x)$ varies.

From equations (7a)–(7c), we can evaluate eigenvalues and eigenfunctions for $H_e + V_{e-rad}$ as a function of x and the field intensity. In order to build the matrix elements for the hamiltonian, we note the following properties: (i) from parity considerations, all diagonal elements of V_{e-rad} are zero, thus $H_{ii} = U_i$; (ii) since the diabatic functions diagonalize the total electronic hamiltonian $H_e(\mathbf{q}, \xi)$, then $H_{ij} = (V_{e-rad})_{ij} = V_{ij;}$ (iii) in our particular case, Ψ_1 and Ψ_2 have the same parity, thence $H_{12} = 0$. We can take the remaining matrix elements V_{13} and V_{23} as variable parameters. In principle, these couplings to the TS will depend on the

U_i-values and the field intensity; for simplicity, we scan their values in the approximation $V_{13} = V_{23}$, and study their effect on the electronic transitions. After all these considerations, the final expression for the hamiltonian matrix is

$$([H_e + V_{e-rad}]_{ij}) = \begin{pmatrix} 0 & 0 & V_{13} \\ 0 & \Delta U_{12} & V_{13} \\ V_{13} & V_{13} & \Delta U_{13} \end{pmatrix}, \tag{8}$$

when the eigenvalues $\varepsilon(x)$ (cf. equation. (5)) are measured relative to $U_1(x)$, and $\Delta U_{12} = U_2 - U_1$, $\Delta U_{13} = U_3 - U_1$. In order to follow the transition from reactant to products, we monitor the lowest eigenvalue $\varepsilon_1(x)$ and its corresponding eigenfunction, with variational coefficients $c_1 = V_{13}c_3/\varepsilon_1$, $c_2 = -V_{13}c_3/(\Delta U_{12} - \varepsilon_1)$, $c_3 = \{1 + [V_{13}/\varepsilon_1]^2 + [V_{13}/(\Delta U_{12} - \varepsilon_1)]^2\}^{-1/2}$, as a function of x. To cover the range from high to low external fields, we scan the coupling in $0.1 \leq V_{13} \leq 30.0$.

We can make an initial analysis of the secular equation associate with equation (8), and estimate the behaviour of the $\{c_i(x)\}$ coefficients for the total quantum state $|\Phi\rangle$. We consider two limit configurations, the reactant-like at $x \approx 0$ and a product-like at $x \gg 1$:

(a) *Reactant-like configurations*: At $x \approx 0$, all energy gaps remain finite, with $\Delta U_{12} = U_2(0)$ and $\Delta U_{13} = U_3(0)$. If the coupling to the external field is small ($V_{13} < 1$), the lowest eigenvalue is estimated as $\varepsilon_1 \approx -(V_{13}^2/U_3) + V_{13}^4[(1/U_3^3) - (1/U_2U_3^2)]$ (For larger V_{13}, no simple expression can be extracted for the ε_1 root). From here, we deduce that the coefficient for the reactant state dominates as

$$|c_1| \approx 1 - V_{13}^2 \left[\frac{1}{U_2U_3} - \frac{1}{2U_3^2} \right], \tag{9a}$$

whereas the product state has a residual contribution of:

$$|c_2| \approx \frac{V_{13}^2}{U_2U_3} + O(V_{13}^3). \tag{9b}$$

The diabatic transition state contributes also near the stationary geometry of the diabatic reactant state as:

$$|c_3| \approx \frac{V_{13}}{U_3} - \frac{V_{13}^3}{2U_3^3}. \tag{9c}$$

Note that the latter contribution, although small, is an order of magnitude larger than $|c_2|$.

(b) *Product-like configurations*: If $x \gg 1$, the energy gaps diverge and we get $\Delta U_{12} \approx -U_1$. If the curvature of the diabatic potential energy for the TS resemble that of the reactant, we also have $|\Delta U_{13}| \ll |\Delta U_{12}|$ for $x \gg 1$. In this limit,

the lowest eigenvalue can be estimated as $\varepsilon_1 \approx \Delta U_{12} + V_{13}^2/\Delta U_{12} + V_{13}^2/\Delta U_{12}^2 < 0$, which produces a dominant product-like total wave function with

$$|c_2| \approx 1 - \frac{V_{13}^2}{2\Delta U_{12}^2}, \tag{10a}$$

for small V_{13} couplings. As in (a), the transition structure $|\Psi_3\rangle$ contributes more at product-like geometries than the diabatic reactant state:

$$|c_1| \approx \frac{V_{13}^2}{\Delta U_{12}^2} + \frac{V_{13}^2 \Delta U_{13}}{\Delta U_{12}^3}, \tag{10b}$$

$$|c_1| \approx |\frac{V_{13}}{\Delta U_{12}} + \frac{V_{13}\Delta U_{13}}{\Delta U_{12}^2}|. \tag{10c}$$

This analysis allows us to draw some conclusions about the total wave function Φ:

(i) The nature of the total quantum state $|\Phi\rangle$ switches as the positive-charge configuration changes, for $V_{13} > 0$. The limits $|c_1(0)| \approx 1$ and $|c_2(0)| \approx 0$ imply $|\Phi\rangle \approx |\Psi_1\rangle$ near $x \approx 0$, whereas the conditions $|c_1(\infty)| \approx 0$ and $|c_2(\infty)| \approx 1$ imply $|\Phi\rangle \approx |\Psi_2\rangle$ for large x values. No change in the wave function can take place if $V_{13} = 0$, in contrast with the adiabatic method.

(ii) For intermediate values of x, we expect a maximum in $|c_3|$. Its position need not coincide with the point at which reactants and products have an equal weight in the total quantum state ($c_1 = c_2$). The latter condition takes place when the corresponding diabatic curves cross ($\Delta U_{12} = 0$), i.e., near the region where the adiabatic BO approximation would fail.

(iii) Our analysis implies that the shift in behaviour from $|\Phi\rangle \approx |\Psi_1\rangle$ to $|\Phi\rangle \approx |\Psi_2\rangle$ is mediated by both the V_{13} value and the diabatic transition state $|\Psi_3\rangle$. Moreover, the fact that $|c_1|$ and $|c_2|$ vary more slowly than $|c_3|$ near the limit geometries, $x \to 0$ and $x \to \infty$, suggests that the transition from $|\Psi_1\rangle$ to $|\Psi_2\rangle$ could be *sharp* as x increases.

4. Electronic transitions mediated by the external field

The exact solution of the model eigenvalue equation as a function of x confirms the previous observations and provides further insight into the electronic transition. Figure 1 shows the behaviour of the effective potential energy of the three-state system (top) and the amplitude in the diabatic states (bottom) in terms of x. The diabatic curves $\{U_i\}$ appear in the top diagram with thin lines.

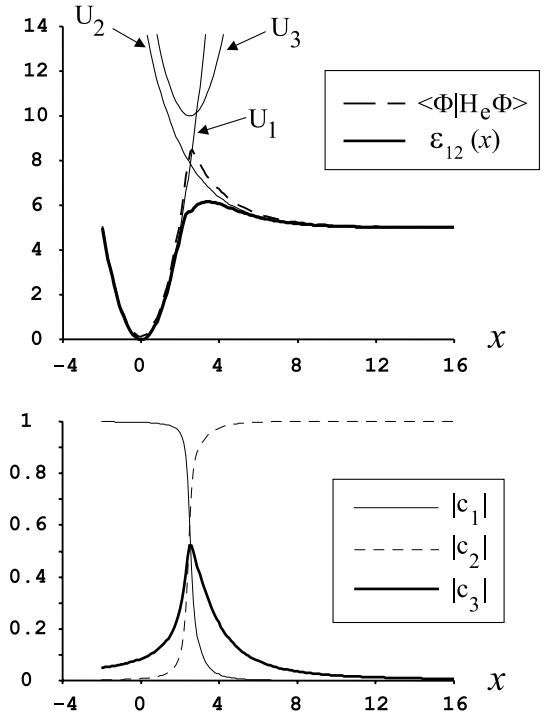

Figure 1. Potential energies (top) and diabatic amplitudes (bottom) for a quantum state of the three-level system, in terms of the elongation x. The U_1, U_2, and U_3 thin lines (top) are the diabatic potentials for reactant, product, and transition states. (If taken in atomic units, the curves will yield over 100 vibrational levels below the dissociation limit in the standard BO approach; see text.) The dotted line is the mean energy of the isolated molecule at the quantum state $|\Phi\rangle$. The thick line is the energy contribution of reactant and product states, ε_{12}. The bottom diagram for the amplitudes shows a sharp transition from $|\Phi > \approx |\Psi_1\rangle$ to $|\Phi\rangle \approx |\Psi_2\rangle$. This transition is mediated by the diabatic transition state, whose contribution maximizes near the $|c_1| = |c_2|$ crossing.

In this case, we have used $k_1 = 2.5$ for the diabatic reactant state and $\Delta_2 = 5$, $k_2 = 10$, $a_2 = 0.5$ for the diabatic product state. (All calculations in this work use always the same parameters for U_2.) The adiabatic TS is characterized by $k_3 = 2.5$, $\Delta_3 = 10$ and $x_3 = 2.5$, and we used a coupling to the external field of $V_{13} = 1.5$. With these parameters, the TS minimum is near the crossing of the reactant and product potential energies ($x \approx 2.51$). The bottom diagram shows a rapid transition in $|c_1|$ and $|c_2|$, in synchrony with a switch in behaviour for $|c_3|$. (The maximum in $|c_3|$ occurs slightly after the crossing $|c_1| = |c_2|$.) The top diagram in figure. 1 shows the total molecular potential energy without the field, $\langle\Phi|H_e\Phi\rangle$, and the partial contribution to it by reactants and products, $\varepsilon_{12} = |c_1|^2 U_1 + |c_2|^2 U_2$. Both functions connect smoothly the diabatic potential energy curves U_1 and U_2, and produce an *apparent barrier* near the diabatic crossing. The "barrier" in ε_{12} is smaller than that for $\langle\Phi|H_e\Phi\rangle$, and it shows a

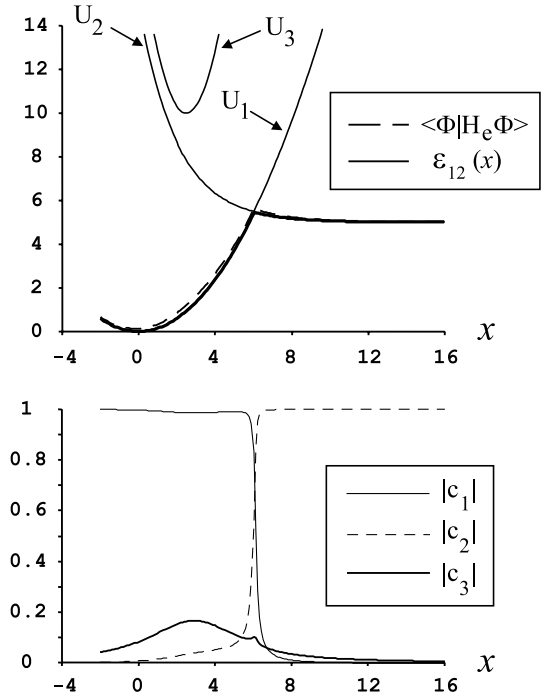

Figure 2. Effective potentials (top) and amplitudes in the basis functions (bottom) for a general quantum state $|\Phi\rangle$. For the symbols, see figure. 1; the only different parameter is the force constant for diabatic reactant state ($k_1 = 0.3$ in figure 2 and $k_1 = 2.5$ in figure 1). The bottom diagram shows also a sharp transition in amplitudes, near the diabatic crossing $U_1 = U_2$. Note, however, that the transition state component $|c_3|$ has only a *secondary* maximum at the transition.

small secondary maximum associated with the maximum in $|c_3|$. Even though we have not used the BO approximation, these effective energies show features that resemble those observed when using adiabatic functions with configuration interaction.

Figure 2 illustrates the effect of shifting the crossing between the diabatic potential energy curves for reactants and products. Here, the parameters for U_i are those in figure. 1, except for a curvature $k_1 = 0.3$ in the reactant state. The same V_{13} coupling is used. In this case, U_1 and U_2 cross at $x \approx 6.05$. As a result of this shift, effective energies $\langle\Phi|H_e\Phi\rangle$ and ε_{12} switch very rapidly between U_1 and U_2 (top diagram). The net result *resembles* an adiabatic "avoided crossing"; in our case, however, there is *no avoided crossing* but instead a rapid change in the quantum state in the presence of the external field. The bottom diagram shows again a sharp transition in $|c_1|$ and $|c_2|$; the transition does not coincide with the absolute maximum in $|c_3|$, but it causes an abrupt *secondary* maximum in $|c_3|$. Note that the absolute maximum in $|c_3|$ causes a local shallow minimum in $|c_1|$.

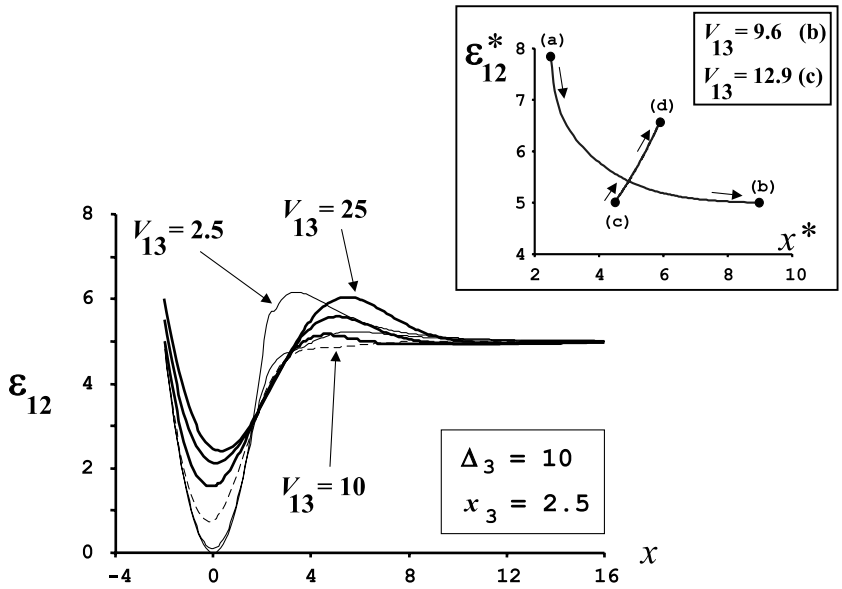

Figure 3. Contribution of diabatic reactant and product states to the effective energy, ε_{12}. Diabatic curves are as in figure. 1; the variation in V_{13} mimics an applied laser field. Values shown: $V_{13} = 2.5$ and 5 (thin lines), 10 (dotted line), and 15, 20, and 25 (thick lines). All curves present a barrier, except for $V_{13} = 10$. The inset gives the barrier position, x^*, and value, ε^*_{12}, for variable V_{13}. The points (a) and (d) denote the lowest and highest V_{13} (0.1 and 30, respectively). Arrows show the direction for increasing V_{13} values. There is *no* barrier between $V_{13} = 9.6$ and $V_{13} = 12.9$.

Although the results in figures 1 and 2 represent well the general behaviour of the three-state model, some interesting features appear for other parameter values. For instance, the apparent energy barrier in ε_{12} depends on the location of the TS and the coupling to the external field. Figure 3 illustrates this property with the diabatic potential energy curves used in figure 1, while scanning the V_{13} coupling between 0.1 and 30.0. For small V_{13} values, we observe the same behaviour as in figure 1, i.e., an apparent barrier at a location x^*, with a value $\varepsilon^*_{12} > U_2(\infty) = 5$. This is the case of the ε_{12} curves for $V_{13} = 2.5$ and $V_{13} = 5$ (thin lines in figure 3). As V_{13} increases, the barrier either *disappears* or becomes *a pair of local maxima and minima* below $U_2(\infty)$. This behaviour corresponds to the case $V_{13} = 10$ in figure 3 (dashed line). Finally, a further increase in V_{13} produces a *late* barrier that shifts as the external field intensity increases. The latter case appears in figure 3 with the curves for $V_{13} = 15, 20,$ and 25 (thick lines). The overall pattern of barrier shift and location is summarized by the top-right inset, which shows the variation in ε^*_{12} and x^* as a function of V_{13}. Starting from point (a) (with $V_{13} = 0.1$), the barrier height diminishes as V_{13} increases along the line (a)→(b). At the critical value $V_{13} = 9.6$, the barrier disappears. It then reappears at $V_{13} = 12.9$, and the barrier's position shifts rapidly with V_{13} following the line (c)→(d).

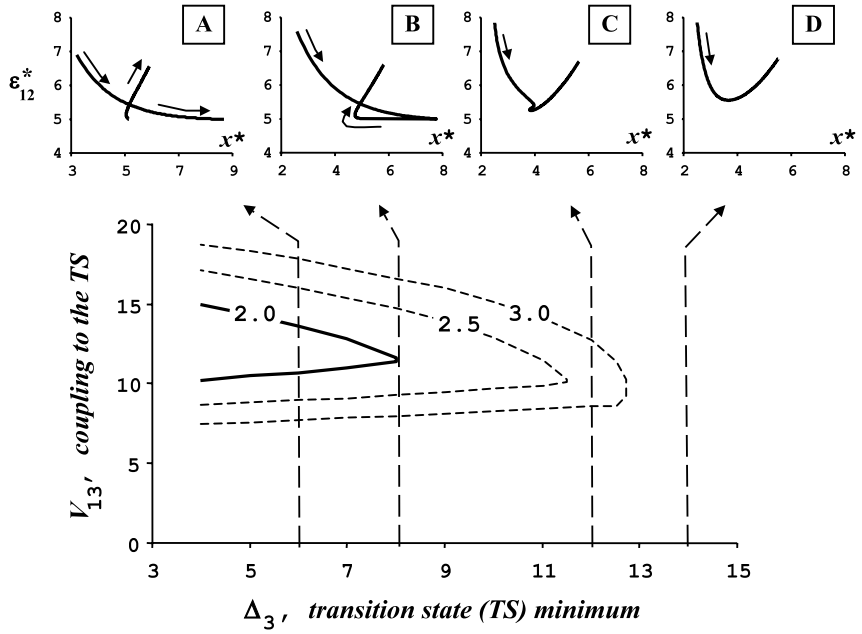

Figure 4. Phase diagram for barriers in the effective energy ε_{12}^*. The bottom diagram shows the barrier regions in (Δ_3, V_{13})-parameter space for various *location* of the TS minimum, x_3. Thus, the thick-line curve in the lower diagram encloses the region with *no barriers* for $x_3 = 2.0$. The two dotted-line curves enclose the regions without barriers for $x_3 = 2.5$ and $x_3 = 3.0$. The top insets give the position and height of the barrier in terms of V_{13} for $x_3 = 2.0$ (cf. inset in figure 3). The A–D diagrams correspond to values of the TS minimum of Δ_3=6, 8, 12, and 14, respectively. Insets are connected with cross sections in the phase diagram by the dashed vertical lines.

If one chooses a different potential energy curve U_3, the critical V_{13} values for an effective barrier will change. To illustrate this, we built a "phase diagram" for the ε_{12} function in terms of a molecular parameter (Δ_3) and an external parameter (V_{13}). On this parameter space, we can locate the locus of all (Δ_3, V_{13})-points where the barrier disappears, for each TS minimum x_3. (The barrier disappears whenever $x^* \to \infty$ or $\varepsilon_{12}^* \to U_2(\infty)$.) The result is shown in figure 4 (main bottom diagram). The curves in (Δ_3, V_{13})-space enclose the regions with *no barrier* for three TS locations, $x_3 = 2$ (curve in thick-line), and $x_3 = 2.5$ and $x_3 = 3$ (curves in dashed lines). The no-barrier region for $x_3 = 3$ encloses that for $x_3 = 2.5$, which in turn encloses that for $x_3 = 2$. The case $x_3 = 3$ represents the maximum extension for a no-barrier zone; for $x_3 > 3$, this region is squeezed towards lower Δ_3 values (data not shown). The four insets on top show the variation in barrier shape (x^* vs. ε_{12}^*) for $x_3 = 2$ and four values of Δ_3. Inset "A" corresponds to $x_3 = 2$ and $\Delta_3 = 6$; the diagram resembles figure 3, where the effective barrier disappears. (The arrows denote the direction for the increase in V_{13}.) Inset "B" corresponds to $x_3 = 2$ and $\Delta_3 = 8$, which

Table 1
Maximum contribution of the diabatic transition state to the total quantum electronic state, as a function of the position and height of the transition state minimum (x_3 and Δ_3, respectively) and the V_{13} coupling. The three columns on the left-hand side half give the maximum $|c_3|$ value (top entry) and its position in the x axis (below, in parenthesis) for a weak coupling ($V_{13} = 0.1$). The columns on the right-hand side give the results corresponding to a strong coupling ($V_{13} = 10$) (see text for a discussion of the trends observed).

	$V_{13} = 0.1$			$V_{13} = 10$		
Δ_3	$x_3 = 2.0$	$x_3 = 2.5$	$x_3 = 3.0$	$x_3 = 2.0$	$x_3 = 2.5$	$x_3 = 3.0$
6	0.996	0.997	0.997	0.728	0.737	0.743
	(2.55)	(2.63)	(2.74)	(2.74)	(2.99)	(3.26)
7	0.971	0.989	0.981	0.715	0.725	0.730
	(2.52)	(2.57)	(2.62)	(2.73)	(2.97)	(3.23)
8	0.261	0.525	0.272	0.703	0.712	0.717
	(2.51)	(2.51)	(2.51)	(2.72)	(2.95)	(3.20)
9	0.082	0.108	0.083	0.690	0.699	0.704
	(2.51)	(2.51)	(2.51)	(2.71)	(2.94)	(3.18)
10	0.046	0.054	0.047	0.677	0.686	0.691
	(2.51)	(2.51)	(2.51)	(2.70)	(2.92)	(3.15)
11	0.032	0.035	0.032	0.664	0.673	0.677
	(2.51)	(2.51)	(2.51)	(2.69)	(2.90)	(3.13)
12	0.024	0.026	0.024	0.651	0.660	0.664
	(2.51)	(2.51)	(2.51)	(2.68)	(2.89)	(3.10)

is just outside the no-barrier region. In this case, the barrier shifts in a complicated manner to and from large x^* values as V_{13} increases. Finally, the "C" and "D" insets show how the barrier behaviour simplifies when moving away from the no-barrier region as Δ_3 increases. In these regions, the effective barrier may be followed by a shallow secondary minimum below $U_2(\infty)$, in addition to the main minimum at $x \approx 0$.

Table 1 completes our analysis with the maximum value of the TS amplitude $|c_3|$. The results use the diabatic U_1 and U_2 curves in figure 1 (which cross at $x \approx 2.51$ and $U_1 = U_2 = 7.86$), over a range of values for Δ_3, x_3, and V_{13}. Table 1 shows the value of max $|c_3|$ (top) and its location in the x axis (below, in parenthesis). We observe the following trends.

(i) At low field intensities ($V_{13} = 0.1$), the quantum state resembles the diabatic transition state (max $|c_3| > 0.97$) whenever the TS minimum is below the diabatic $U_1 = U_2$ crossing (i.e., $\Delta_3 < 8$). Note that the TS contribution maximizes at $x = 2.5$, i.e., when the diabatic curve U_3 is centred near the $U_1 = U_2$ crossing. This behaviour recalls the standard adiabatic BO picture where the TS is a saddle point on top of an energy barrier [16]. In our case, this is not a required condition, but it highlights the TSs dominant role in mediating

the electronic transition from $|\Phi\rangle \approx |\Psi_1\rangle$ to $|\Phi\rangle \approx |\Psi_2\rangle$. This behaviour is maintained for low V_{13} values as Δ_3 increases, although the max $|c_3|$ value decreases if the TS is higher in energy. For sufficiently large Δ_3 values, the maximum weight of the TS is found at the $U_1 = U_2$ crossing, regardless of x_3.

(ii) At high field intensities ($V_{13} = 10$), the diabatic TS remains the main contribution to the quantum state for all Δ_3 and x_3. In this case, max $|c_3|$ is not the largest when the TS minimum is near the $U_1 = U_2$ crossing. Moreover, max $|c_3|$ decreases as the TS becomes higher in energy, but the result does not depend very strongly on whether the TS minimum is above or below the crossing of the diabatic reactant and product states. Note also that max $|c_3|$ is always located at $x > 2.51$, i.e., away from the $U_1 = U_2$ crossing. We can conclude that, for large V_{13}, the molecule is essentially "dressed" in the field, and *its behaviour is much less dependent on features of the isolated molecular system*.

5. Conclusions and final remarks

We have shown how transitions in quantum state can be represented in a generalized diabatic approach. Within the present GED method, the electronic diabatic states $\Psi_s(\mathbf{q})$ do not depend on the configuration of the embedded array of classical positive charges, yet they determine the single attractor associated with each relevant chemical species. The general quantum state $|\Phi\rangle$ of a nonisolated molecular system appears thus as a linear superposition in the $\Psi_s(\mathbf{q})$ basis set; information on the electromagnetic field (e.g., a laser field) and the positive-charge geometry is only found in the linear coefficients. The resulting representation for $|\Phi\rangle$ can be regarded as akin to a multiconfigurational wave function.

In this approach, chemical reactions occur as transitions in a nonisolated system. In the case of a closed-shell, there is also the additional requirement of an open-shell TS which couples the diabatic states of reactant and product in the presence of an electromagnetic field. Note that an actual excitation to the TS is not required to produce a transition, nor is a change of the diabatic states with the spatial configuration of the nuclear charges. The emerging picture is one where, by the presence of the external field, one can "borrow" energy from the TS and then "use" it, so to speak, to adapt the total quantum state from a reactant-like to a product-like function. This transition is found to be *sharp*, in the sense that it involves a small region of the configurational space for the positive charges. The net process can be better likened to a "vertical tunneling" from reactant to products via the TS, rather than a conventional horizontal transmission through a potential energy barrier. This interpretation should remain valid if one later adds the dynamics of nuclear masses.

The GED approach provides an appealing physical description. Covalent bond breaking emerges as a Franck–Condon process by using the tools employed to study general quantum transitions, i.e., the superposition principle

and an external field. Moreover, our simple three-state model allows us to recover familiar entities without resorting to the adiabatic approximation: energy barriers and shallow double minima are found as properties of the effective potential energy for particular values of the model parameters. Adaptations of the three-state model to study other types of chemical reactions will be discussed elsewhere.

Acknowledgments

G.A.A. thanks the Department of Physical Chemistry (Uppsala University) for its hospitality. This research was supported by NSERC (Canada) and the Canada Research Chairs' Program.

References

[1] L.J. Butler, Annu. Rev. Phys. Chem. 49 (1998) 125.
[2] V. May and O. Kühn, *Charge and Energy Transfer Dynamics in Molecular Systems* (VCH–Wiley, Berlin, 2000).
[3] F.T. Smith, Phys. Rev. 179 (1969) 111.
[4] D.R. Yarkony, Rev. Mod. Phys. 68 (1996) 985.
[5] H. Nakamura and D. Truhlar, J. Chem. Phys. 115 (2001) 10353.
[6] H. Nakamura and D. Truhlar, J. Chem. Phys. 117 (2002) 5576.
[7] E. Deumens, A. Diz, R. Longo and Y. Öhrn, Rev. Mod. Phys. 66 (1994) 917.
[8] H. Gabriel and K. Taulbjerg, Phys. Rev. A 10 (1974) 741.
[9] O. Tapia and P. Braña, J. Mol. Struct. (Theochem) 580 (2002) 9.
[10] O. Tapia, in: A. Hernández-Laguna, J. Maruani, R. McWeeny and S. Wilson (Eds.), *Quantum Systems in Chemistry and Physics, Vol. 2: Advanced Problems and Complex Systems* (Kluwer, Dordrecht, 2000, pp. 195–212).
[11] M. Baer, Chem. Phys. Lett. 35 (1975) 112; Chem. Phys. 15 (1976) 49.
[12] T. Pacher, L.S. Cederbaum and H. Köppel, J. Chem. Phys. 89 (1988) 7367.
[13] L.M. Andersson, F. Burmeister, H.O. Karlsson and O. Goscinski, Phys. Rev. A 65 (2001) 12705.
[14] T. Kato, Trans. Am. Math. Soc. 70 (1951) 195; Trans. Am. Math. Soc. 70 (1951) 212.
[15] O. Tapia, J. Mol. Struct. (Theochem.) 537 (2001) 89.
[16] J. Michl and V. Bonačič-Koutecký, *Electronic Aspects of Organic Photochemistry*, (Wiley, New York, 1990, pp. 148–156).